Available online at www.sciencedirect.com

SCIENCE DIRECT

Biochimica et Biophysica Acta 1721 (2005) 16–26

BIOCHIMICA ET BIOPHYSICA ACTA
BBA

http://www.elsevier.com/locate/bba

Phosphorylation modulates the alpha-helical structure and polymerization of a peptide from the third tau microtubule-binding repeat

Jesús Mendieta[a,b], Miguel A. Fuertes[a], Rani Kunjishapatham[c], Ismael Santa-María[a], Francisco J. Moreno[a], Carlos Alonso[a], Federico Gago[b], Victor Muñoz[c], Jesús Avila[a,*], Félix Hernández[a]

[a]*Centro de Biología Molecular "Severo Ochoa" CSIC/UAM, Fac. Ciencias, Universidad Autónoma de Madrid, Cantoblanco, 28049 Madrid, Spain*
[b]*Departamento de Farmacología, Universidad de Alcalá, 28871 Alcalá de Henares, Madrid, Spain*
[c]*Department of Chemistry and Biochemistry and Center for Biomolecular Structure and Organization, University of Maryland, College Park, Maryland 20742, USA*

Received 22 July 2004; received in revised form 10 September 2004; accepted 22 September 2004
Available online 19 October 2004

Abstract

Paired helical filaments (PHFs) isolated from patients with Alzheimer's disease (AD) mainly consist of the microtubule-associated protein tau in a hyperphosphorylated form. It has been found that PHFs are the first example of pathological protein aggregation associated with formation of α-helices [Biochemistry (2002) 41, 7150–5]. In an effort to investigate the interplay between phosphorylation and the putative role of short regions of alpha-helix in the polymerization of tau, we have focused on the region of tau encompassing residues 317 to 335. This region is able to form protein fibrils in vitro and has two serines that are often found phosphorylated in PHFs. Using trifluoroethanol as an indicator of the alpha-helix, we find that the stability of the alpha-helix conformation is enhanced by phosphorylation. Circular dichroism data show that the phosphorylated peptide in water presents a content in alpha-helix similar to the unphosphorylated peptide at 40% of trifluoroethanol. Phosphorylation also stimulates the effect of juglone in promoting the in vitro polymerization. Furthermore, Fourier transformed infrared spectroscopy of samples of phosphorylated peptide polymerized with juglone renders a spectrum with maxima at ~1665 and ~1675 cm^{-1}, which are suggestive of a mixture of turns and alpha-helix conformations. Our results provide a direct mechanistic connection between phosphorylation and polymerization in tau. The connection between phosphorylation and polymerization appears to involve formation of alpha-helix structure.

Keywords: Phosphorylation; Tau; Alzheimer's disease; Circular dichroism; Molecular dynamic; Fourier transformed infrared spectroscopy

1. Introduction

Alzheimer's disease (AD) is characterized by the presence of two aberrant structures, senile plaques and neurofibrillary tangles (NFT). The main component of NFT is the paired helical filaments (PHFs) [1], which are mainly comprised of the protein tau in an abnormally phosphorylated status [2]. Tau was first isolated as a microtubule associated protein, since it co-purifies with microtubules and stabilizes them (for a review, see Ref. [3]). The binding of tau to microtubules was found to be through specific microtubule binding domains (MBDs). These domains are three or four imperfectly repeated sequences of 31 or 32 residues located in the C-terminal half of the tau molecule [4–6]. In AD, tau binds with lower affinity to microtubules and it self-aggregates into aberrant structures, probably helped by other molecules (for a review, see Ref. [7]). Proteolytic digestion of PHFs shows that the amino- and

* Corresponding author. Tel.: +34 91 497 8443; fax: +34 91 497 4799.
E-mail address: javila@cbm.uam.es (J. Avila).

0304-4165/$ - see front matter © 2004 Elsevier B.V. All rights reserved.
doi:10.1016/j.bbagen.2004.09.009

carboxyl-terminal termini of tau protein form a coat around the filaments, while the MBDs form the core of the PHFs [8–10].

After the discovery that tau protein was the main component of PHFs, several attempts were made to obtain PHFs in vitro. It was reported that tau protein purified from brain extracts is able to aggregate in vitro although only at high concentrations [11–14]. This observation suggested that some other molecules might contribute to tau assembly. Sulfo-glycosaminoglycans (sGAG) received special attention mainly because they are present in the NFT [15,16]. In vitro, tau polymerization is facilitated by sGAG [17,18], with heparin being the most studied example. Similarly, other polyanions such as RNA [19] and polyglutamic acid [18,20] also favor tau aggregation. Fatty acids or fatty acid-like molecules [21–23] and the lipid peroxidation product, 4-hydroxy-2-nonenal (HNE) [24], enhance the polymerization of tau in vitro. Recently, several quinones, (e.g., juglone, coenzyme Q10 and menadione) have been described to induce the in vitro polymerization of tau into fibrillar structures [25]. The fact that peptides encompassing amino acids 306–311 [26] and 317–335 [18] polymerize into fibrillar aggregates suggests that the minimal region of tau able to self-assemble is localized in the third microtubule-binding repeat.

The role of phosphorylation in the self-assembly of tau is a fundamental question in the study of AD and other tauopathies. It has been suggested that phosphorylation of some specific tau sites may be a prerequisite for its assembly [27,28]. Some of these sites occur, indeed, in the PHF core-forming MBD domain. Serine-324 is part of the third microtubule-binding repeat and is phosphorylated by PKA [29]. Phosphorylation of serine-324 generates a putative consensus site for GSK-3β [30]. GSK-3β is identical to tau protein kinase I (TPK I), an enzyme that was identified in brain extracts because it could phosphorylate tau in vitro [31]. GSK-3β is one of the best candidate enzymes for generating the hyperphosphorylated tau that is characteristic of PHFs (for a review, see Ref. [32]). However, in vitro experiments to test the effect of phosphorylation on tau self-assembly have shown varied results, presumably reflecting slight differences in experimental conditions. In some experiments phosphorylated tau displays a decreased propensity to aggregate [33], whereas in other conditions the aggregation propensity increases [24]. Thus, discrepancy in the results can be due to differences in tau protein concentration or in the status of tau phosphorylation. In fact, phosphorylation of some regions can probably inhibit aggregation, while phosphorylation of other regions can induce tau polymerization. Compounds such as HNE [24] and several quinones [25] catalyze the formation of fibrillar aggregates of phosphorylated tau peptides, but fail to have an observable effect if the peptides are in a non-phosphorylated form.

Another fundamental question refers to the molecular structure of tau protein in the PHF particle. The current view is that pathological protein aggregation must involve formation of β-sheet structure giving rise to the typical amyloid fibrils [34]. The discovery of α-helix structure in ex vivo PHFs [35] indicates that PHFs are not a typical case of amyloidosis. The role of α-helix structure in PHF formation is also supported by recent work showing that the region implicated in forming the core of PHFs (i.e., MBD domain) becomes very α-helix upon addition of the helix-promoting agent TFE [36–38]. The observation of electron diffraction patterns characteristic of crossed-beta structure in samples of Down-syndrome PHFs [39] and the identification of β-sheet structure in tau fibrils polymerized in vitro with heparin [39,40] support the role of β-structure in PHF formation.

The fact that phosphorylation of tau occurs in sites of the same region that is involved in forming the core of PHFs has led to suggestions that phosphorylation controls assembly. However, no mechanistic model of the interplay between phosphorylation and assembly has been proposed. Here, we attempt to address these issues using a peptide corresponding to tau region 317–335 as the simplest model system. Our results reveal a higher helical propensity of region 317–335 upon phosphorylation. Phosphorylation also facilitates the aggregation of region 317–335 into fibrillar polymers grown in the presence of juglone. FTIR analysis of these polymers indicates the presence of a mixture of turns and helical conformations, and the absence of β-structure. This is in sharp contrast to the structure of the polymers formed by a shorter peptide (306 VQIVYK 311, [26]) in the presence of heparin.

2. Materials and methods

2.1. Materials

5-Hydroxy-1,4-naphthoquinone (juglone, Ref. H4, 700-3) was obtained from Aldrich. (γ-^{32}P) ATP was purchased from Amersham. ATP was purchased from Boehringer-Mannheim. The catalytic subunit of cAMP-dependent protein kinase (PKA, P 2645) and recombinant GSK-3β were purchased from Sigma. 2,2,2-Trifluoroethanol was from Fluka (TFE, Ref 91683). The peptide corresponding to residues 317–335 (1/2R peptide) of Tau protein (Fig. 1; KVTSKCGSLGNIHHKPGGG), the same peptide prephosphorylated (1/2R-P; KVTS(P)KCGS(P)LGNIHHKPGGG), and the peptide corresponding to residues 306–311 (VQIVYK) were chemically synthesized by Neosystem S.A. (Strasbourg, France).

2.2. Peptide phosphorylation

The phosphorylation of 1/2R peptide was performed as previously described [25]. Briefly, purified PKA and 4 μg of peptide were used in a 12-μl total volume of buffer

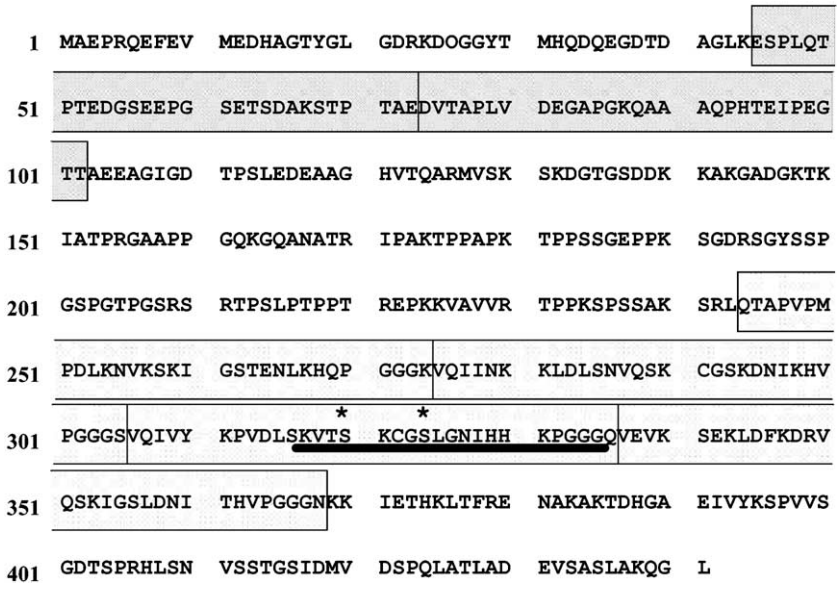

Fig. 1. Tau domains present in the largest CNS tau isoform. Shaded box, exons 2 and 3. Doted box; the four microtubule-binding repeats. The 1/2R peptide is underlined. Asterisks indicate the Ser residues phosphorylated in the 1/2R-P peptide. Numbering of the amino acids is according to the longest human CNS tau isoform of 441 amino acids.

solution containing 50 μM ATP. The cAMP kinase protein (100 ng/reaction) was performed in 50 mM Tris–HCl, pH 7.5, 10 mM $MgCl_2$, 1 mM EGTA, 1 mM EDTA and 1 μM okadaic acid buffer, at 37 °C. After 2 h of incubation, samples were boiled for 5 min to inactivate PKA. Then, 0.1 μg/μl recombinant GSK-3β and [γ-^{32}P]ATP (20 μM–1 μCi assay) were added. After 30 min, SDS-PAGE sample buffer was added to stop the reaction and samples were electrophoresed on a 15% SDS gel. The gels were vacuum-dried and autoradiographed. LiCl (20 mM) was used as specific GSK-3β inhibitor.

2.3. Molecular dynamics simulations

The peptide in α-helical conformation was built using the biopolymer module of the Insight II program (Accelrys). Atomic charges for phospho-Ser residues were obtained with RESP program [41] so as to fit the molecular electrostatic potential calculated at 6-31G* level of theory using the ab initio quantum mechanics program Gaussian98 [42].

Each molecular system was neutralized by the addition of the appropriate number of chloride ions and immersed in a rectangular box of TIP3P water molecules. Each water box extended 8 Å away of any solute atom, and the cutoff distance for non-bonded interaction was 10 Å. Periodic boundary conditions were applied and electrostatic interactions were represented using the smooth particle mesh Ewald method with a grid spacing of ~1 Å. Unrestrained molecular dynamics simulations (4 ns) at 298 ° K and 1 atm were run for unphosphorylated, monophosphorylated and biphosphorylated peptides using the SANDER module of AMBER. SHAKE was applied to all bonds involving hydrogens, and an integration step of 2 fs was used.

2.4. CD measurements

Far-UV CD spectra were recorded using a Jasco spectropolarimeter, model 600 (Jasco Europe SLR) fitted to a thermostated cell holder at a temperature of 25 °C interfaced to a NESLAB RTE-100 water bath. The scan rate was 50 nm min^{-1}, the time response was 2s, and the CD spectra were the mean of five accumulations for each run. A cell of 1-mm light path was used. Solutions of 4×10^{-2} mM of peptide with different proportions of TFE were scanned at room temperature. The results were expressed in term of mean residue ellipticity, $[\theta]$, in units of deg cm^2 $dmol^{-1}$.

CD spectra were smoothed with Savitsky–Golay smooth function and arranged in a data matrix of ellipticity D (nR,nC), with as many nR rows as number CD spectra were recorded at each TFE proportion, and as many nC columns as wavelength was scanned during the run.

The more probable number of components is investigated simply from inspection of the magnitude of singular values of matrix D (Singular Value Decomposition). An initial estimation of the evolution of the components is obtained by Evolving Factor Analysis (EFA) [43]. From this estimation, a constrained Alternating Least Squares (ALS) optimization algorithm [44] is started to try to recover the correct set of concentration profiles and individual spectroscopic responses. This recovery is based on the assumption that the instrumental responses of the chemical contributions are bilinear, i.e., they can be expressed in a matrix equation like:

$$D = CS + E$$

where C is the matrix describing how the chemical contributions change (e.g., species distribution) with the

number of rows equal to the number of experimental measured CD spectra, and the number of columns equal to the number of proposed chemical contributions. S is the matrix of the pure individual spectroscopic contributions with the number of rows equal to the number of proposed chemical contributions and with the number of columns equal to the number of scanned wavelength. E is the residual matrix containing the variance not explained by C and S.

The ALS optimization procedure is started solving iteratively the equation previously given from an estimation of the concentration profiles and constraining at each stage of the iterative optimization the concentration profiles to be nonnegative. Details about the implementation of this method have been applied to study of conformational changes in protein previously [45,46].

The content of secondary structure was evaluated by least squares fitting deconvolution using as basis spectra corresponding to α -helix, β-sheet and random coil [47].

2.5. Fourier transformed infrared spectroscopy

Fourier infrared absorption spectra were obtained in aqueous solution and dry film using a Digilab Excalibur FTS 3000 FTIR spectrometer equipped with a Harrick ConcentraIR horizontal multiple reflection (ATR) accessory. For each spectrum 1024 interferograms at 4 cm^{-1} resolution were co-added, and then Fourier transformed using triangular apodization. Samples of each polymerization reaction were dried, resuspended in water, and then analyzed against a background of water.

2.6. Isolation of the paired helical filaments

Brain samples, supplied by Dr. Ravid (Netherlands Brain Bank, The Netherlands), from AD patients were used to isolate PHFs by following the procedure described previously [48]. The PHF samples were visualized by electron microscopy as described below.

2.7. Assembly of tau peptides into filaments

Filaments were grown by vapor diffusion in hanging drops in the standard way used for protein crystallization as previously indicated [11,49]. In a typical experiment, 4 μg of peptides was resuspended in 20 μl of buffer A (0.1 M MES, pH 6.4, 0.5 mM $MgCl_2$ and 2 mM EGTA) containing 50 mM NaCl plus DMSO (final concentration 0.5%) or juglone (2 mM). Filaments were obtained after incubation for 4 days at 4°C. The samples were visualized by electron microscopy.

2.8. Electron microscopy

Electron microscopy was performed after adsorption of the samples to electron microscopy carbon-coated grids and stained with 2% uranyl acetate for 1 min. Transmission electron microscopy was performed in a JEOL Model 1200EX electron microscope operated at 100 kV.

3. Results

3.1. Molecular dynamics simulation

The relation between phosphorylation of tau protein and its aberrant assembly into PHFs [27,28], as well as the helical tendency of a peptide derived from the third MBD [36], strongly suggests that phosphorylation can be able to alter the secondary structure of some regions of tau protein. This structural modification can be an important issue in the aggregation process.

Molecular dynamics (MD) simulation is a useful tool to study the effects of covalent changes on peptide or protein structures. To test the hypothesis that phosphorylation could modify the stability of the helical structure of some MBD regions, we performed molecular dynamics simulations of the 1/2R peptide (Fig. 1). Simulations were carried out in the presence of explicit water molecules using as the starting conformation a peptide in which all residues presented the Φ and ψ angles corresponding to a theoretical α-helix (-57° and -47° respectively). Trajectories of 4 ns were performed for an unphosphorylated peptide, the peptide phosphorylated at residue Ser324, and the peptide phosphorylated at both Ser320 and Ser324. The stability of the putative α-helix structure was monitored by the root mean square deviation (RMSD) of Cα atoms of all peptide residues using as reference the theoretical α-helix. Due to the presence of a Pro and three Gly residues, which destabilize the α-helix at the C-terminal extreme of the peptide, the RMSD of Cα atoms as far as residue 330 was also monitored. Fig. 2a shows that the helical structure of the unphosphorylated peptide progressively disorganized during the simulation. This disorganization affects the whole extension of the peptide as shown by RMSD of the peptide without the C-terminal Pro–Gly-rich fragment. The α-helix structure of the Ser324-phosphorylated peptide presents more stability along the entire trajectory. The N-terminal fragment of the peptide was very stable during the firsts 2 ns. For the rest of the simulation this fragment becomes moderately unstable, but considering the whole extension of the peptide, a high helical structure was kept during the entire trajectory (Fig. 2b). The N-terminal fragment of the biphosphorylated peptide was highly stable during all the simulation (Fig. 2c). The moderate disorganization of the α-helix observed during the trajectory seems to be due to the C-terminal Pro–Gly-rich fragment of the peptide.

Fig. 2d shows the ribbon representation of a theoretical α-helix and the final structures corresponding to the three peptides used in the simulations. The α-helix structure of the unphosphorylated peptide was broken just in the proximity of the phosphorylatable Ser residues, while both phosphorylated peptides keep a high helical structure at the

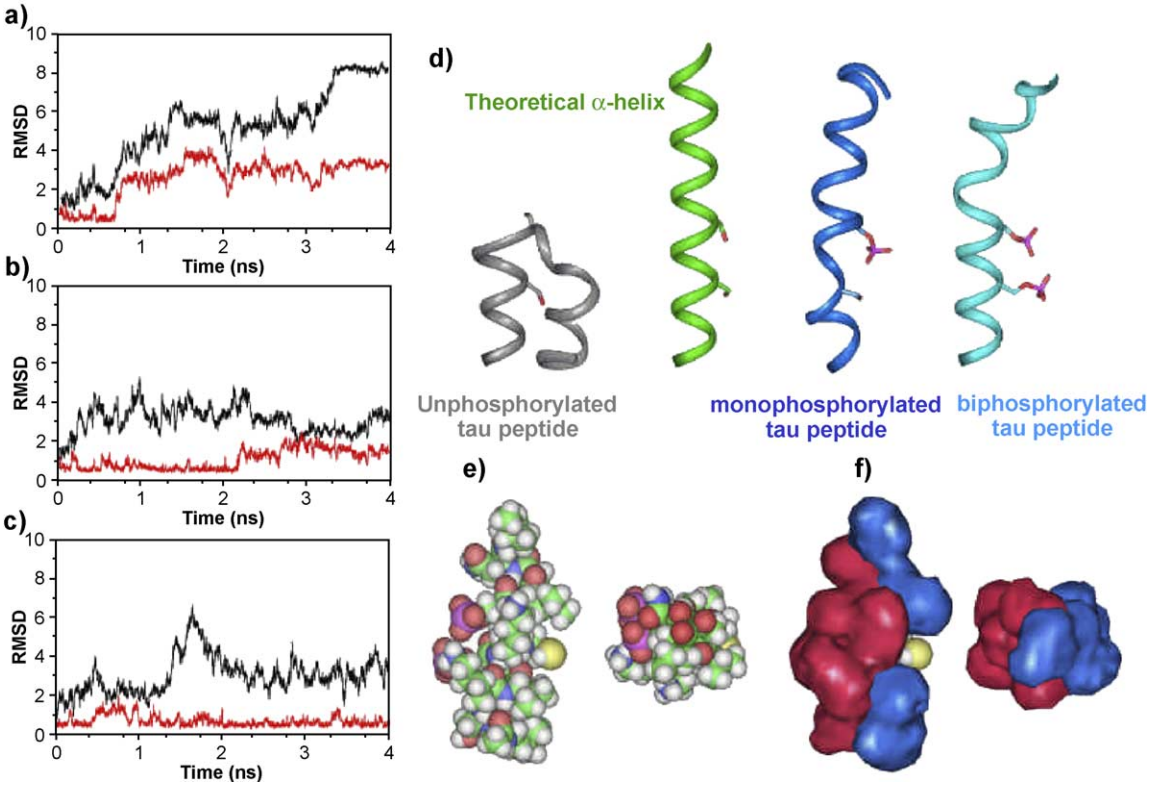

Fig. 2. (a) Root mean square deviations (RMSD) of Cα atoms for all residues (black lines) and residues until the His 330 for the unphosphorylated, (b) the monophosphorylated and (c) the biphosphorylated 1/2R peptide. (d) Ribbon representation of the conformation of the initial theoretical α-helix (green ribbon), and the final structures for the unphosphorylated (grey ribbon), the monophosphorylated (blue ribbon) and the biphosphorylated 1/2R peptide (cyan ribbon). (e) Representation of the atoms of the final structure obtained after molecular dynamics simulations of the phosphorylated peptide in a lateral view, and in the direction of the axe of the helix. (f) Similar views as in (e) but the atoms have been replaced by a surface formed by polar residues (red) and apolar residues (blue).

end of the simulations. Interestingly, in the case of the monophosphorylated peptide, the α-helix was slightly distorted in the proximity of the phopho-Ser324 and the phosphorylatable Ser320. The biphosphorylated peptide keeps a structure very close to the theoretical α-helix in the N-terminal fragment, including the two phospho-Ser, and the deviation of the helical structure was restricted to the Pro–Gly-rich fragment. The high stability of the biphosphorylated peptide could be due to strong interaction between the negatively charged phosphorylated residues and the Lys317 and Lys321 basic residues (not shown in Fig. 2d).

Our results suggest that the stability of the putative helical structure of the 1/2R peptide is highly influenced by its phosphorylation state. The α-helix seems to be more stable when peptide is completely phosphorylated at Ser residues than in the non-modified peptide.

3.2. Tau 1/2R is phosphorylated by the priming kinase PKA and then by GSK-3β

To demonstrate that the 1/2R peptide is phosphorylated in both serines, we focused our investigation in PKA and GSK-3. PKA is able to phosphorylate serine-324 [29] and then generate a consensus site recognize by GSK-3 [30]. That motif is present in the peptide 1/2R prephosphorylated by PKA in serine-324 (Fig. 1). Thus, we prephosphorylate the peptide with or without PKA and unlabelled "cold" ATP, and later on with GSK-3β and [γ-^{32}P]ATP (Fig. 3). The results demonstrate that the third MBD is modified by PKA and GSK-3, suggesting that PKA acts as a priming kinase for GSK-3. In fact, if the 1/2R peptide is not primed by PKA, GSK-3β is not able to incorporate ^{32}P in the substrate. As a control, the effect of 20 mM LiCl, an inhibitor of GSK-3, is also shown.

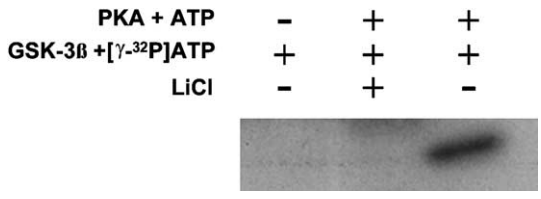

Fig. 3. GSK-3β phosphorylates peptide 1/2R. GSK-3β phosphorylates a primed peptide prephosphorylated by PKA with "cold" ATP, while unprimed peptide is not phosphorylated by GSK-3β. As a control, GSK-3β was also incubated with 20 mM LiCl. The phosphorylation reactions were carried out as described in Materials and methods.

3.3. CD spectra of 1/2R and 1/2R-P in water and TFE solutions

Our results suggest that phosphorylation of residues Ser320 and Ser324 increases the stability of a putative α-helix secondary structure of a peptide derived from the third MBD. A high helical content for a non-modified analogue peptide at TFE 100% (v/v) has been found [36]. With the aim of obtaining experimental support for our MD simulation results, we study the ability of TFE to induce helical structure in the biphosphorylated 1/2R peptide compared with the non-modified peptide. TFE is frequently used as a medium for determining the propensity to acquire α-helix structure for polypeptides by CD spectroscopy, showing a relation between such propensity and the concentration at which the conformational change occurs [50].

Fig. 4 shows a 3D plot of the evolution of CD spectra corresponding to the unphosphorylated and the phosphorylated peptides. In both cases, spectra obtained in the absence of TFE were compatible with a very high content of random coil corresponding to a short peptide derived from an unfolded protein in native conditions. However, the behavior of the both peptides in the presence of TFE was different from usually observed in other peptides with helical propensity. No sharp transition between random coil and α-helix spectra was found, but the shape of the spectrum changes softly to reach a plateau at intermediate concentrations of TFE. Only at higher concentration of TFE the spectrum corresponding to α-helix appears. Such a behavior of the peptide makes it difficult to find significant differences in the helical propensity of the peptide in relation with the phosphorylation state. With the purpose to obtain all the structural information on the changes in the CD spectra, Factor Analysis techniques were applied to the study of the process as previously proposed [45,46]. CD data were arranged in a data matrix form (see Materials and methods), and singular value decomposition was performed in order to discriminate if the data can be explained by a linear combination of two CD spectra. The singular value analysis of the data matrices corresponding to the unphosphorylated and the biphosphorylated peptides shows that in both cases only two components are necessary to explain the variation of the data, all other components are at the level of the background noise (data not shown). Furthermore, the singular value analysis of a matrix generated with the two sets of data can also be explained with two components (Fig. 5a). The result suggests that no additional components other than that present in the unphosphorylated peptide are necessary to explain the effect of phosphorylation in the peptide conformation.

An initial estimation of the concentration profiles corresponding to the two components can be obtained from evolving factor analysis and then the spectra for the components and the contribution of each to the spectra obtained at different concentrations of TFE were obtained using the ALS optimization algorithm (see Materials and methods). Fig. 5b shows the results of the factor analysis treatment of the matrix generated with the two sets of data. The spectra of the first component are in agreement with a high content of random coil. The relation among the ellipticity at 209 and 222 nm in the second component suggests a higher content of α-helix. However, the evolution of the contribution of these two components shows a different profile for both peptides (Fig. 5c–d). In the case of the unphosphorylated peptide the first component is predominant at low concentration of TFE and decreases until 40% of TFE to reach a series of spectra in which the contributions of the two components are of the same order. Only for TFE concentration higher than 80% the second component becomes predominant. In the case of the biphosphorylated peptide the contribution of the second component is higher even at low concentration of TFE and becomes predominant at concentration higher than 50%.

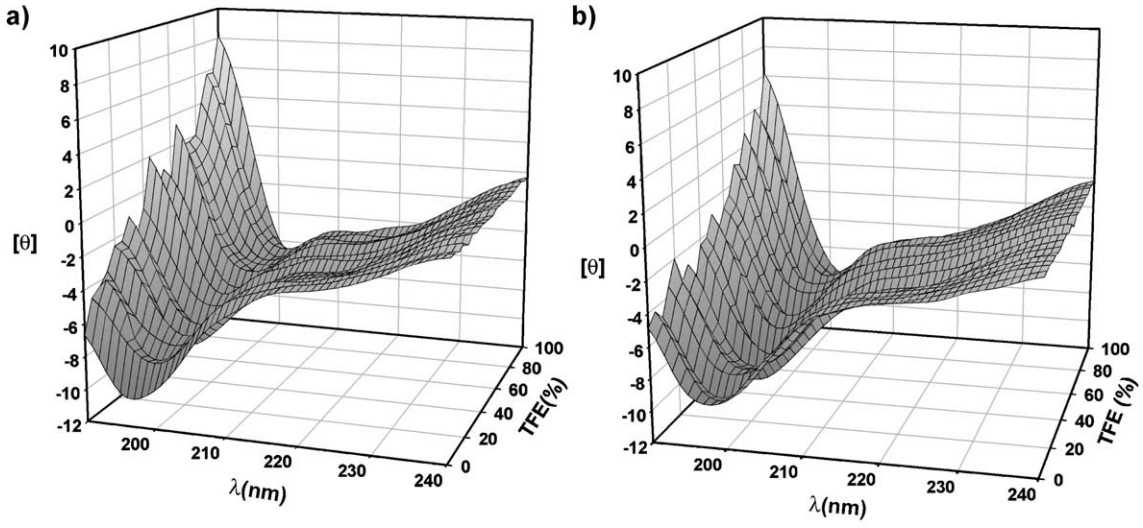

Fig. 4. Mesh 3D plot of the evolution of the CD spectra of 1/2R (a) and 1/2R-P (b) with increasing concentration of TFE.

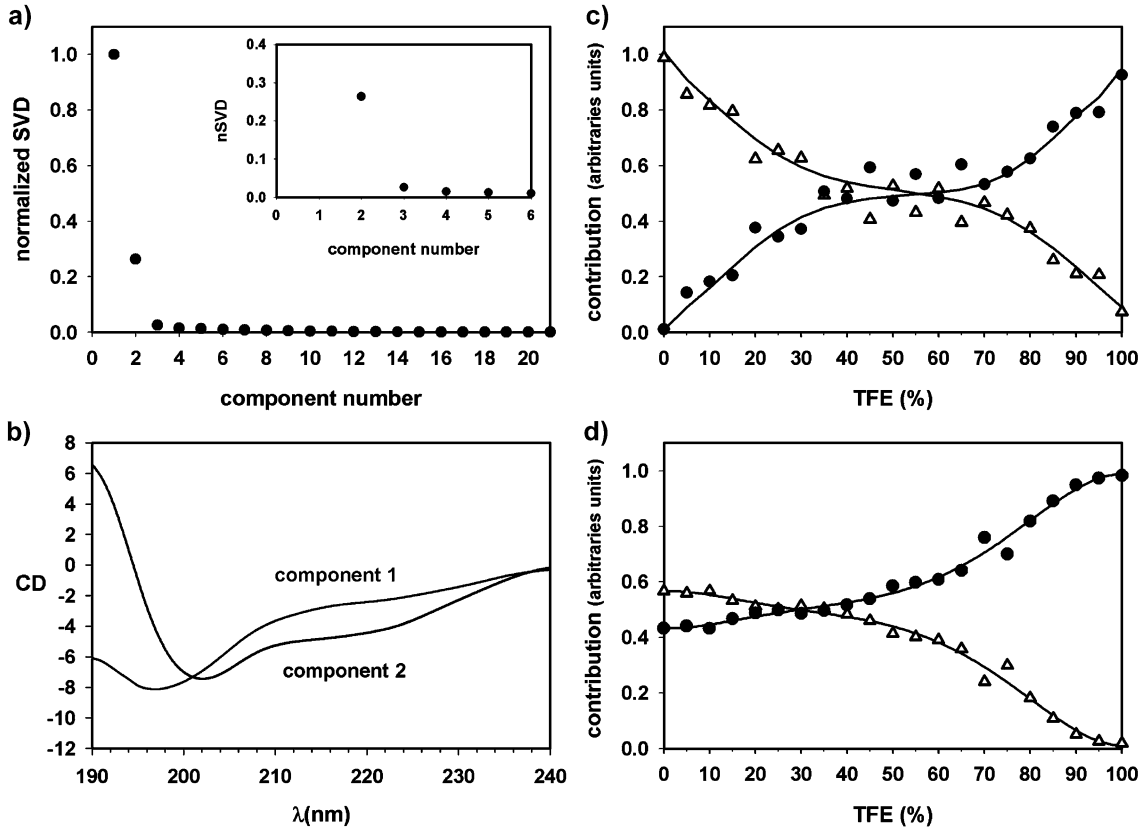

Fig. 5. (a) Singular value decomposition of the CD data matrix generated with the two sets of data from Fig. 4. (b) CD spectra of the two components obtained by Multivariated Curve Resolution of the data matrix. The evolution of the contribution of the components versus the concentration of TFE is shown for the unphosphorylated peptide (c) and the phosphorylated peptide (d).

More information about the conformational changes in the peptides can be obtained after deconvolution of the spectra of the two components to the basic spectra corresponding to α-helix, β-sheet and random coil structures [47]. Once the secondary structure content of the spectra corresponding to the principal components has been estimated, the proportion of α-helix, β-sheet and random coil present at each TFE concentration can be calculated taking into account the concentration profiles obtained by the ALS optimization method (Fig. 6). In both cases the peptides show a high content of random coil conformation which is not affected by the concentration of TFE. For the unphosphorylated peptide, at low TFE concentration the content of β-sheet decreases softly while the α-helix content increases in the same proportion. At intermediate concentration of TFE the secondary structure of the peptide does not change. For a concentration higher than 60% the β-sheet is substituted by α-helix to reach a content of this secondary structure around 45% and only residual content of β-sheet. In the case of the biphosphorylated peptide, the content of secondary structure at low concentrations of TFE was similar to that found in the case of the non-modified peptide at intermediate concentration. The β-sheet to α-helix transition is initiated at 40% of TFE, a lower concentration than in the case of the unmodified peptide.

These results suggest a higher α-helical propensity of the biphosphorylated peptide in relation to the unphosphorylated one, confirming the results obtained by MD simulations.

3.4. Polymerization of the peptides in the presence of juglone

We have analyzed the propensity to self-assemble of both peptides in the presence of juglone, a quinone that has been described to induce tau polymerization in vitro [25]. No polymers were observed in the absence of juglone (data not shown), while bona fide filaments were obtained only when the peptide 1/2R-P was used (Fig. 7). The filaments obtained (Fig. 7C–D) have width and length similar to those of PHFs isolated from AD patients brains (Fig. 7A).

3.5. FTIR analysis of polymerized samples

To investigate the molecular structure of the peptide in the polymeric structures, we measured the bulk FTIR spectrum of samples of each peptide after the polymerization reactions. Fig. 8a shows the amide I–amide II FTIR spectrum of a sample of peptide 317–335 biphosphorylated polymerized in the presence of juglone (dashed line), and a sample of a shorter peptide from the same region (306

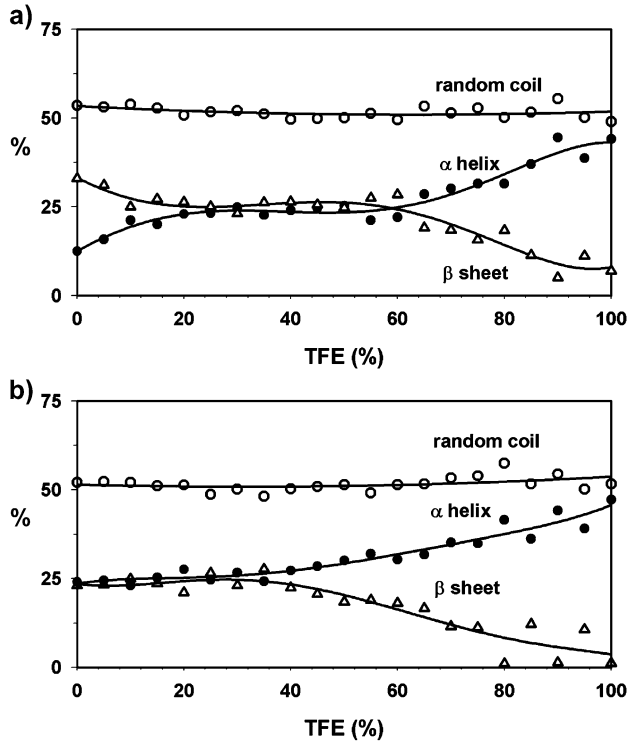

Fig. 6. The evolution of the contribution of α-helix, β-sheet and random-coil versus the concentration of TFE for the unphosphorylated (a) and the phosphorylated peptide (b).

VQIVYK 311; Ref. [26]) polymerized with heparin (continuous line). Fig. 8b shows the second derivative spectrum of the data shown in Fig. 8a using the same color-coding. The short peptide polymerized with heparin has a broad amide I spectrum with a maximum at ~1670 cm^{-1} and a distinct shoulder at 1620 cm^{-1}. The second derivative spectrum reveals that the shoulder at 1620 cm^{-1} is produced by a sharp peak that corresponds to formation of crossed-beta structure [51]. The maximum at 1670 cm^{-1} is due to a broader band characteristic of turns and/or beta. Samples of peptide 317–335 polymerized with juglone have a very different FTIR spectrum. The maximum is still found at ~1670 cm^{-1}, but the band at 1620 cm^{-1} is totally absent. The absence of the 1620 cm^{-1} band permits to unambiguously assign the peak at 1670 cm^{-1} to turn conformations. The second derivative spectrum reveals that together with the major band at 1670 cm^{-1}, there are two other bands of lower intensity at 1685 and 1655 cm^{-1}, which can be assigned to turn and α-helix conformations, respectively [52].

4. Discussion

Knowing what regions of the protein tau are involved in its aggregation into aberrant filaments and what molecular structure is induced by aggregation are critical steps towards understanding the mechanisms involved in the pathological aggregation of tau. Tau protein is a natively unfolded protein, but PHFs isolated from brain of people with AD have α-helical structure [35]. The concomitant appearance of α-helix structure and aggregation of tau indicates that the two processes are intertwined. Secondary structure prediction algorithms suggest that the MBD region of tau has significant propensity to form α-helices [7]. By carrying out molecular dynamics simulations we find that the propensity of a short segment of tau protein located in the third MBD (residues 317 to 335, the peptide 1/2R) to populate α-helix conformations seems to be higher when the peptide is phosphorylated in two serine sites. We have experimentally confirmed this prediction by analyzing the secondary structure of peptide 317–335 in non-phosphorylated and biphosphorylated forms using circular dichroism as a function of increasing amounts of TFE. This analysis shows that the highest α-helix population is for the biphosphorylated peptide, and the lowest for the non-phosphorylated one. Furthermore, the assembly of these peptides in the presence of quinones is strongly facilitated by phosphorylation. The CD spectrum of the biphosphorylated peptide in the absence of TFE is similar to the spectrum of the unphosphorylated peptide at low concentration of TFE (<10% [TFE] >40%). Interestingly, the polymerization of a similar non-phosphorylated peptide is favored in similar TFE concentrations [38].

Tau protein purified from brain extracts or recombinant tau is able to aggregate in vitro at high concentrations of protein [11–14]. However, to study the mechanism of tau aggregation using the full-length tau molecule is difficult because some regions of the protein act as inhibitors of tau polymerization. Furthermore, even if full-length tau obtained by recombinant means was used, this protein does not mimic the phosphorylation state of tau molecules comprising PHFs. Therefore, in spite of the growing amount of data suggesting that different domains of the protein may have different secondary structures (for a review, see Ref. [7]), we have decided to approach the problem studying these factors in small fragments of tau. Fragments from the tubulin-binding motif of tau can assemble into filaments in vitro. We have previously reported that the peptide 1/2R (contained in the third MBD) is possibly the minimal segment of that region able to grow in vitro into filaments in the presence of heparin [18,53]. This suggests that the ability of tau for self-assembly could be localized in a short sequence of amino acids present in the tubulin-binding repeats of the tau molecule, as it has been previously suggested [11,14].

Our analysis is germane to two open questions in the field of PHF formation. The first question refers to the contribution of α-helix/β-sheet to the structure of in vivo PHF filaments. The second question is related to the contribution of phosphorylation to the formation of PHFs. In respect to the first point, the third tubulin-binding repeat can be separated in three segments: the short peptide 306 VQIVYK 311, which has been found to aggregate in vitro [26] in agreement with the conclusions of a comprehensive study on the aggregational properties of short peptides [54]; a peptide comprising the residues 314 DLSKVTS 320,

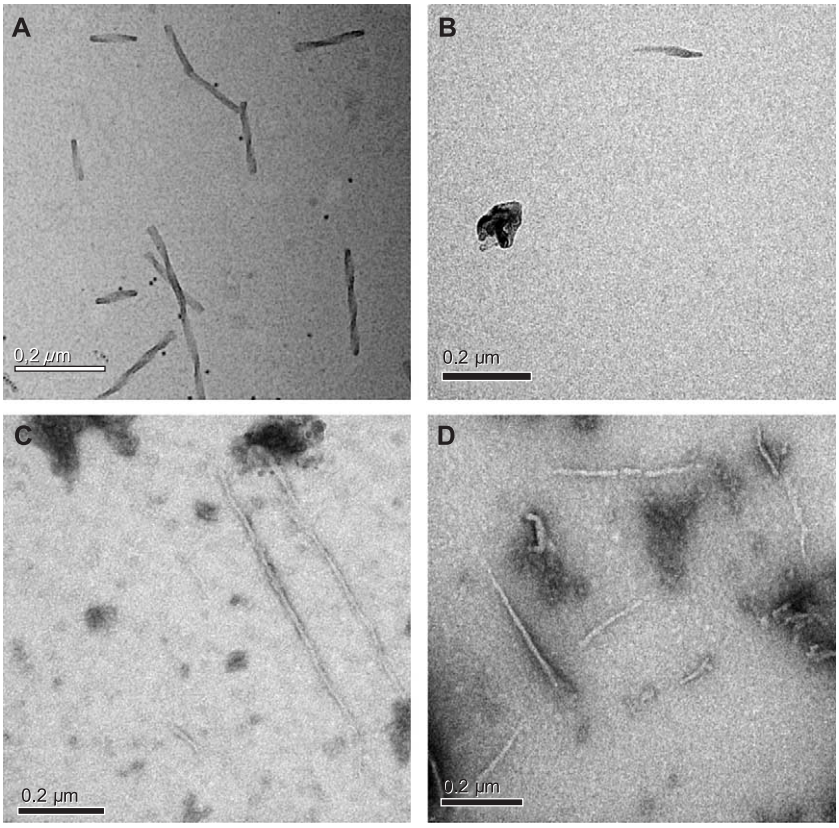

Fig. 7. Electron microscopy of negatively stained filaments. (A) PHFs isolated from human samples. (B–D) Morphology of filaments assembled in the presence of juglone by using unphosphorylated peptide (B) or phosphorylated peptide (C–D). The samples were treated as described in Materials and methods. Scale bar represents 200 nm.

which seems to also play an important role in the polymerization process of tau [55]; finally, the peptide 1/2R (KVTSKCGSLGNIHHGKPGGG), which is also able to self-assemble into fibrillar aggregates in vitro [18,53] while it displays significant α-helix propensity (our data and [36,56]). Thus, the assembly of full-length tau is expected to involve contributions from each of these regions from the third MBD. Interestingly, it has been recently described that the isolated third MBD assembles more efficiently than the second MBD, although both domains have similar amino acid sequences [37]. All these data suggest a key role for the third MBD in tau polymerization. In another recent publication it has been reported that assembly of the fourth MBD is most favored in concentrations of TFE ranging from 10% to 30% [38]. Based on this observation, the authors propose that the aggregation competent state involves a conformation with intermediate α-helical content [38]. Our results add new and important information to the question of the contribution of α-helix to the polymerization of tau protein (see Ref. [7]). We have here confirmed previous results [36,37] indicating that the third MBD populates α-helix conformations in TFE. We also find that the peptide 1/2R biphosphorylated has a higher propensity to form α-helical structures than the unphosphorylated one.

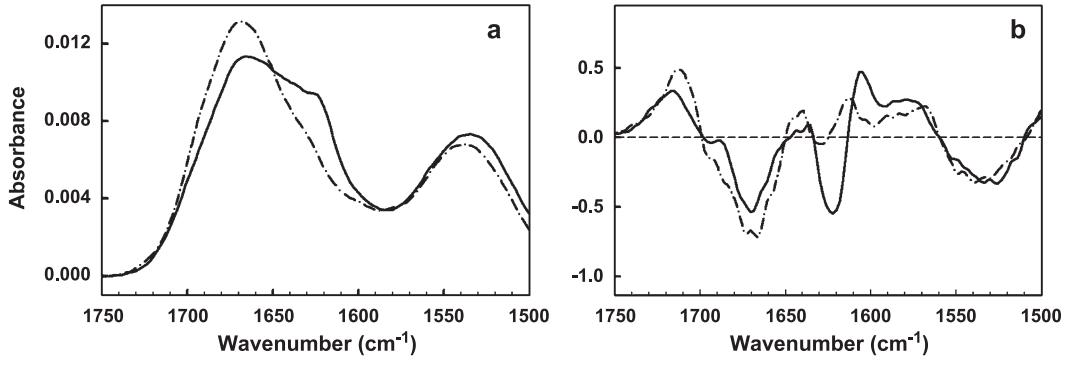

Fig. 8. FTIR analysis of samples of polymerized peptides. (a) Amide I–amide II region of the infrared spectrum of peptide 317–335 polymerized with juglone (dashed line), and peptide 306 VQIVYK 311 polymerized with heparin (continuous line). (b) Second derivative of the amide I–amide II spectra shown in a.

Furthermore, the FTIR spectrum of the juglone-induced polymers of the phosphorylated peptide indicates that the peptide is forming a mixture of turn and α-helical conformations. These results are in agreement with the idea of the intermediate conformations being the aggregation competent state. Moreover, our results clearly show that the molecular structure of these aggregates is very different from that of the short peptide 306–311 polymerized with heparin. Thus, our findings support the idea that polymerization of MBD in the presence of juglone occurs through formation of partially α-helical conformations, which are stimulated by phosphorylation. The amphipathic nature of the peptide 1/2R (Fig. 2e–f) suggests a mechanism for polymerization in which the interaction between two amphipathic α-helices is the first step in polymerization. It can be matter of discussion if, after the interaction of the phosphorylated third MBD, PHF formation is facilitated in vivo by only some of the compounds that induce tau assembly in vitro, such as quinones and HNE. Another interesting issue is whether other tau domains are necessary for the tau assembly into bona fide filaments. In any event, the higher propensity to form α-helical structure of 1/2R biphosphorylated peptide supports a physiological role for phosphorylation and α-helix formation.

Acknowledgements

We are grateful to Elena Langa and Raquel Cuadros for laboratory technical assistance. This work was supported by grants from Fundación La Caixa, Spanish CICYT, Comunidad de Madrid, Fundatión Lilly, and by an institutional grant from Fundación Ramón Areces.

References

[1] M. Kidd, Paired helical filaments in electron microscopy of Alzheimer's disease, Nature 197 (1963) 192–193.
[2] I. Grundke-Iqbal, K. Iqbal, Y.C. Tung, M. Quinlan, H.M. Wisniewski, L.I. Binder, Abnormal phosphorylation of the microtubule-associated protein tau (tau) in Alzheimer cytoskeletal pathology, Proc. Natl. Acad. Sci. U. S. A. 83 (1986) 4913–4917.
[3] J. Avila, J.J. Lucas, M. Perez, F. Hernandez, Role of tau protein in both physiological and pathological conditions, Physiol. Rev. 84 (2004) 361–384.
[4] G. Lee, N. Cowan, M. Kirschner, The primary structure and heterogeneity of tau protein from mouse brain, Science 239 (1988) 285–288.
[5] M. Goedert, M.G. Spillantini, M.C. Potier, J. Ulrich, R.A. Crowther, Cloning and sequencing of the cDNA encoding an isoform of microtubule-associated protein tau containing four tandem repeats: differential expression of tau protein mRNAs in human brain, EMBO J. 8 (1989) 393–399.
[6] A. Himmler, Structure of the bovine tau gene: alternatively spliced transcripts generate a protein family, Mol. Cell. Biol. 9 (1989) 1389–1396.
[7] T.C. Gamblin, R.W. Berry, L.I. Binder, Modeling tau polymerization in vitro: a review and synthesis, Biochemistry 42 (2003) 15009–15017.
[8] H. Ksiezak-Reding, S.H. Yen, Structural stability of paired helical filaments requires microtubule-binding domains of tau: a model for self-association, Neuron 6 (1991) 717–728.
[9] M. Goedert, M.G. Spillantini, N.J. Cairns, R.A. Crowther, Tau proteins of Alzheimer paired helical filaments: abnormal phosphorylation of all six brain isoforms, Neuron 8 (1992) 159–168.
[10] C.M. Wischik, M. Novak, P.C. Edwards, A. Klug, W. Tichelaar, R.A. Crowther, Structural characterization of the core of the paired helical filament of Alzheimer disease, Proc. Natl. Acad. Sci. U. S. A. 85 (1988) 4884–4888.
[11] R.A. Crowther, O.F. Olesen, M.J. Smith, R. Jakes, M. Goedert, Assembly of Alzheimer-like filaments from full-length tau protein, FEBS Lett. 337 (1994) 135–138.
[12] E. Montejo de Garcini, J. Avila, In vitro conditions for the self-polymerization of the microtubule-associated protein, tau factor, J. Biochem. (Tokyo) 102 (1987) 1415–1421.
[13] E. Montejo de Garcini, J.L. Carrascosa, I. Correas, A. Nieto, J. Avila, Tau factor polymers are similar to paired helical filaments of Alzheimer's disease, FEBS Lett. 236 (1988) 150–154.
[14] H. Wille, G. Drewes, J. Biernat, E.M. Mandelkow, E. Mandelkow, Alzheimer-like paired helical filaments and antiparallel dimers formed from microtubule-associated protein tau in vitro, J. Cell Biol. 118 (1992) 573–584.
[15] M.G. Spillantini, M. Tolnay, S. Love, M. Goedert, Microtubule-associated protein tau, heparan sulfate and alpha-synuclein in several neurodegenerative diseases with dementia, Acta Neuropathol. (Berl) 97 (1999) 585–594.
[16] G. Perry, S.L. Siedlak, P. Richey, M. Kawai, P. Cras, R.N. Kalaria, P.G. Galloway, J.M. Scardina, B. Cordell, B.D. Greenberg, et al., Association of heparan sulfate proteoglycan with the neurofibrillary tangles of Alzheimer's disease, J. Neurosci. 11 (1991) 3679–3683.
[17] M. Goedert, R. Jakes, M.G. Spillantini, M. Hasegawa, M.J. Smith, R.A. Crowther, Assembly of microtubule-associated protein tau into Alzheimer-like filaments induced by sulfated glycosaminoglycans, Nature 383 (1996) 550–553.
[18] M. Perez, J.M. Valpuesta, M. Medina, E. Montejo de Garcini, J. Avila, Polymerization of tau into filaments in the presence of heparin: the minimal sequence required for tau–tau interaction, J. Neurochem. 67 (1996) 1183–1190.
[19] T. Kampers, P. Friedhoff, J. Biernat, E.M. Mandelkow, E. Mandelkow, RNA stimulates aggregation of microtubule-associated protein tau into Alzheimer-like paired helical filaments, FEBS Lett. 399 (1996) 344–349.
[20] P. Friedhoff, A. Schneider, E.M. Mandelkow, E. Mandelkow, Rapid assembly of Alzheimer-like paired helical filaments from microtubule-associated protein tau monitored by fluorescence in solution, Biochemistry 37 (1998) 10223–10230.
[21] D.M. Wilson, L.I. Binder, Free fatty acids stimulate the polymerization of tau and amyloid beta peptides. In vitro evidence for a common effector of pathogenesis in Alzheimer's disease, Am. J. Pathol. 150 (1997) 2181–2195.
[22] T.C. Gamblin, M.E. King, J. Kuret, R.W. Berry, L.I. Binder, Oxidative regulation of fatty acid-induced tau polymerization, Biochemistry 39 (2000) 14203–14210.
[23] C.N. Chirita, M. Necula, J. Kuret, Anionic micelles and vesicles induce tau fibrillization in vitro, J. Biol. Chem. 278 (2003) 25644–25650.
[24] M. Perez, R. Cuadros, M.A. Smith, G. Perry, J. Avila, Phosphorylated, but not native, tau protein assembles following reaction with the lipid peroxidation product, 4-hydroxy-2-nonenal, FEBS Lett. 486 (2000) 270–274.
[25] I. Santa-María, F. Hernández, C. Pérez-Martín, J. Avila, F.J. Moreno, Quinones facilitate the self-assembly of the phosphorylated tubulin binding region of tau into fibrillar polymers, Biochemistry 43 (2004) 2888–2897.
[26] M. von Bergen, P. Friedhoff, J. Biernat, J. Heberle, E.M. Mandelkow, E. Mandelkow, Assembly of tau protein into Alzheimer paired helical filaments depends on a local sequence motif ((306)VQIVYK(311))

forming beta structure, Proc. Natl. Acad. Sci. U. S. A. 97 (2000) 5129–5134.
[27] C. Bancher, C. Brunner, H. Lassmann, H. Budka, K. Jellinger, G. Wiche, F. Seitelberger, I. Grundke-Iqbal, K. Iqbal, H.M. Wisniewski, Accumulation of abnormally phosphorylated tau precedes the formation of neurofibrillary tangles in Alzheimer's disease, Brain Res. 477 (1989) 90–99.
[28] W. Gordon-Krajcer, L. Yang, H. Ksiezak-Reding, Conformation of paired helical filaments blocks dephosphorylation of epitopes shared with fetal tau except Ser199/202 and Ser202/Thr205, Brain Res. 856 (2000) 163–175.
[29] C.W. Scott, R.C. Spreen, J.L. Herman, F.P. Chow, M.D. Davison, J. Young, C.B. Caputo, Phosphorylation of recombinant tau by cAMP-dependent protein kinase. Identification of phosphorylation sites and effect on microtubule assembly, J. Biol. Chem. 268 (1993) 1166–1173.
[30] S. Frame, P. Cohen, R.M. Biondi, A common phosphate binding site explains the unique substrate specificity of GSK3 and its inactivation by phosphorylation, Mol. Cell 7 (2001) 1321–1327.
[31] K. Ishiguro, A. Shiratsuchi, S. Sato, A. Omori, M. Arioka, S. Kobayashi, T. Uchida, K. Imahori, Glycogen synthase kinase 3 beta is identical to tau protein kinase I generating several epitopes of paired helical filaments, FEBS Lett. 325 (1993) 167–172.
[32] H. Eldar-Finkelman, Glycogen synthase kinase 3: an emerging therapeutic target, Trends Mol. Med. 8 (2002) 126–132.
[33] A. Schneider, J. Biernat, M. von Bergen, E. Mandelkow, E.M. Mandelkow, Phosphorylation that detaches tau protein from microtubules (Ser262, Ser214) also protects it against aggregation into Alzheimer paired helical filaments, Biochemistry 38 (1999) 3549–3558.
[34] L.C. Serpell, M. Sunde, C.C. Blake, The molecular basis of amyloidosis, Cell. Mol. Life Sci. 53 (1997) 871–887.
[35] M. Sadqi, F. Hernandez, U. Pan, M. Perez, M.D. Schaeberle, J. Avila, V. Munoz, Alpha-helix structure in Alzheimer's disease aggregates of tau-protein, Biochemistry 41 (2002) 7150–7155.
[36] K. Minoura, K. Tomoo, T. Ishida, H. Hasegawa, M. Sasaki, T. Taniguchi, Amphipathic helical behavior of the third repeat fragment in the tau microtubule-binding domain, studied by (1)H NMR spectroscopy, Biochem. Biophys. Res. Commun. 294 (2002) 210–214.
[37] K. Minoura, T.M. Yao, K. Tomoo, M. Sumida, M. Sasaki, T. Taniguchi, T. Ishida, Different associational and conformational behaviors between the second and third repeat fragments in the tau microtubule-binding domain, Eur. J. Biochem. 271 (2004) 545–552.
[38] S. Hiraoka, T.M. Yao, K. Minoura, K. Tomoo, M. Sumida, T. Taniguchi, T. Ishida, Conformational transition state is responsible for assembly of microtubule-binding domain of tau protein, Biochem. Biophys. Res. Commun. 315 (2004) 659–663.
[39] S. Barghorn, P. Davies, E. Mandelkow, Tau paired helical filaments from Alzheimer's disease brain and assembled in vitro are based on beta-structure in the core domain, Biochemistry 43 (2004) 1694–1703.
[40] J. Berriman, L.C. Serpell, K.A. Oberg, A.L. Fink, M. Goedert, R.A. Crowther, Tau filaments from human brain and from in vitro assembly of recombinant protein show cross-beta structure, Proc. Natl. Acad. Sci. U. S. A. 100 (2003) 9034–9038.
[41] P. Cieplak, W. Cornell, C. Bayly, P. Kollman, Application of the multimolecule and multiconformational RESP methodology to biopolymers: charge derivation for DNA, RNA and proteins, J. Comput. Chem. 16 (1995) 1357–1377.
[42] M.J. Frisch, G.W. Trucks, H.B. Schlegel, G.E. Scuseria, M.A. Robb, J.R. Cheeseman, V.G. Zakrzewski, J.A. Montgomery Jr., R.E. Stratmann, J.C. Burant, S. Dapprich, J.M. Millam, A.D. Daniels, K.N. Kudin, M.C. Strain, O. Farkas, J. Tomasi, V. Barone, M. Cossi, R. Cammi, B. Mennucci, C. Pomelli, C. Adamo, S. Clifford, J. Ochterski, G.A. Petersson, P.Y. Ayala, Q. Cui, K. Morokuma, D.K. Malick, A.D. Rabuck, K. Raghavachari, J.B. Foresman, J. Cioslowski, J.V. Ortiz, B.B. Stefanov, G. Liu, A. Liashenko, P. Piskorz, I. Komaromi, R. Gomperts, R.L. Martin, D.J. Fox, T. Keith, M.A. Al-Laham, C.Y. Peng, A. Nanayakkara, C. Gonzalez, M. Challacombe, P.M.W. Gill, B.G. Johnson, W. Chen, M.W. Wong, J.L. Andres, M. Head-Gordon, E.S. Replogle, J.A. Pople, Gaussian 98, Gaussian: Pittsburgh, PA 1998.
[43] H. Gampp, M. Maeder, C. Meyer, A.D. Zuberbuhler, Calculation of equilibrium constants from multiwavelength spectroscopic data model-free least-square refinement by use of evolving factor analysis, Talanta 33 (1986) 943–951.
[44] R. Tauler, Multivariate Curve resolution applied to second order data, Chemometr. Intell. Lab. Syst. 30 (1995) 133–146.
[45] J. Mendieta, H. Folque, R. Tauler, Two-phase induction of the nonnative alpha-helical form of beta-lactoglobulin in the presence of trifluoroethanol, Biophys. J. 76 (1999) 451–457.
[46] J. Mendieta, M.S. Diaz-Cruz, M. Esteban, R. Tauler, Multivariate curve resolution: a possible tool in the detection of intermediate structures in protein folding, Biophys. J. 74 (1998) 2876–2888.
[47] Y.H. Chen, J.T. Yang, K.H. Chau, Determination of the helix and beta form of proteins in aqueous solution by circular dichroism, Biochemistry 13 (1974) 3350–3359.
[48] S.G. Greenberg, P. Davies, A preparation of Alzheimer paired helical filaments that displays distinct tau proteins by polyacrylamide gel electrophoresis, Proc. Natl. Acad. Sci. U. S. A. 87 (1990) 5827–5831.
[49] M. Arrasate, M. Perez, R. Armas-Portela, J. Avila, Polymerization of tau peptides into fibrillar structures. The effect of FTDP-17 mutations, FEBS Lett. 446 (1999) 199–202.
[50] M.K. Luidens, J. Figge, K. Breese, S. Vajda, Predicted and trifluoroethanol-induced alpha-helicity of polypeptides, Biopolymers 39 (1996) 367–376.
[51] A.L. Fink, S. Seshadri, R. Khurana, K.A. Oberg, in: B.R. Singh (Ed.), Infrared Analysis of Peptides and Proteins, Principles and Applications, ACS Symposium Series, vol. 750, 2000.
[52] S. Krimm, in: B.R. Singh (Ed.), Infrared Analysis of Peptides and Proteins, Principles and Applications, ACS Symposium Series vol. 750, 2000.
[53] M. Perez, M. Arrasate, E. Montejo De Garcini, V. Munoz, J. Avila, In vitro assembly of tau protein: mapping the regions involved in filament formation, Biochemistry 40 (2001) 5983–5991.
[54] M. Lopez De La Paz, K. Goldie, J. Zurdo, E. Lacroix, C.M. Dobson, A. Hoenger, L. Serrano, De novo designed peptide-based amyloid fibrils, Proc. Natl. Acad. Sci. U. S. A. 99 (2002) 16052–16057.
[55] A. Abraha, N. Ghoshal, T.C. Gamblin, V. Cryns, R.W. Berry, J. Kuret, L.I. Binder, C-terminal inhibition of tau assembly in vitro and in Alzheimer's disease, J. Cell Sci. 113 (Pt. 21) (2000) 3737–3745.
[56] R.W. Berry, A. Abraha, S. Lagalwar, N. LaPointe, T.C. Gamblin, V.L. Cryns, L.I. Binder, Inhibition of tau polymerization by its carboxy-terminal caspase cleavage fragment, Biochemistry 42 (2003) 8325–8331.